Experimental comparison of resolution & pattern fidelity in single- and double-layer planar lens lithography

David O. S. Melville* **and Richard J. Blaikie†**

MacDiarmid Institute for Advanced Materials and Nanotechnology,

Department of Electrical and Computer Engineering,

University of Canterbury, Christchurch, New Zealand.

(Dated: October 28, 2005)

An experimental comparison of the performance of single- and double-layer planar lens lithography (PLL) has been carried out. A direct comparison is made with a single 50nm silver lens and a double silver lens with two 30nm layers. Sub-diffraction-limited features have been imaged in both cases, with dense grating periods down to 145nm and 170nm for the single- and double-layered stacks, respectively. For the same total thickness of silver the resolution limit is qualitatively better for a double layer stack. However, pattern fidelity is reduced in the double layer experiments due to increased surface roughness. Finite-difference time-domain simulations are also presented to back up the experimental results.

OCIS codes: 110.2990-Image formation theory, 110.5220-Photolithography, 160.4760-Optical properties, 260.1960-Diffraction theory, 310.6860-Thin films, optical properties

*Electronic address: dom15@elec.canterbury.ac.nz

†Author to whom correspondence should be addressed: r.blaikie@elec.canterbury.ac.nz

1. Introduction

One of the most important tools equipping the semiconductor industry was, and still is, optical lithography. Optical lithography's characteristic advantages of cheap, parallel, and repeatable performance gave manufacturers the required economic foot-hold to develop and maintain the industry. However, the struggle to push optical lithography to higher resolution performance is moving the technique away from its strengths, involving more complexity and cost than ever before. New cost-effective methods are needed to overcome the constraining factors in optical lithography, in particular to take the technique past the diffraction-limit without the huge expense. The key to this may lie in the area of plasmonics.

Since Pendry proposed the perfect lens theory in 2000[1] there has been huge interest in the area, amounting to extensive theory, simulation, and experimentation efforts[2]. Pendry predicted that the near-field of a source could be amplified and refocused by a slab of negative index material to reconstruct a sub-diffraction-limited image. This idea built on a 30-year-old theory that propagating waves were also focused by such a slab[3]. Furthermore, Pendry's suggestion of a silver superlens under UV light exposure gave solid direction for sub-100nm super-resolution imaging. Initial work on planar lens lithography (PLL), showing that silver could image features at the i-line wavelength of a mercury lamp[4], has been recently added to with conclusive proof of sub-diffraction-limited imaging[5,6], confirming Pendry's controversial theory. The two experimental demonstrations are similar in many respects, with both using imaging into a photo resist layer. The distinct difference is that our technique[5] is compatible with subsequent pattern transfer, whereas the method of Fang *et al.*[6] is not, so it cannot be used as a lithography process.

Although PLL does not provide better resolution than a contact lithography regime, it is however capable of producing similar resolution at a set distance from the lensing layer[7]. This allows the possibility of sub-diffraction-limited imaging without the need for resist-to-mask contact, which can damage the mask.

Recent work has suggested that dividing a lossy silver slab into multiple layers could improve resolution when comparing setups with the same total thickness[8]. It was suggested that this could lead to a near-field imaging lens that is more resilient to manufacturing imperfections. It is the goal of this work to test this idea for the optical near-field with a multiple-layer silver lens using our developed PLL technique.

The next section gives an overview of our experimental method, as well as a summary

of the limitations in our fabrication processes. The experimental results are then described and analysed giving an insight into the reality of a multi-layered lens before Finite-difference time-domain simulations are performed to back up the experimental results. Finally, conclusions about the system are made.

2. Experimental method

The experimental technique, providing repeatable super-resolution imaging results in an optical lithography environment, is based on previous work describing conformable-contact lithography[9,10]. These methods use flexible membranes under vacuum to ensure intimate contact between an object and an imaging layer. Our experimental setups for single- and double-layer planar lens lithography are shown in Fig 1. A tungsten mask is patterned onto a conformable glass coverslip, before additional spacer (PMMA or SiO_2) and silver layers are deposited. The PLL mask is then attached to a supporting structure and brought into contact with a photosensitive imaging layer. The process steps are briefly described below, while full details can be found in Ref[5].

An accurately determined gap between the bottom of the silver and the imaging layer is extremely important for the success of PLL. This is assured by building conformable masks on flexible glass coverslips, which are either 100 or 200μm thick. The thinner the coverslip the more it will conform to deviations in the imaging layer, allowing the silver-to-image-layer gap to be set by a final spacer layer. However, thinner coverslips are also more prone to breakages. Tungsten features are created by sputtering tungsten onto the coverslips (see Table 7 for deposition parameters) before creating a poly(methylmethacrylate) (PMMA) etch mask with an electron beam lithography (EBL) tool and reactive ion etching (RIE) the result (see table 7 for RIE parameters). Grating patterns have been created with periods from 5μm down to 100nm, as well as isolated features and line pairs, for testing the resolution of the process.

Next, the additional PLL layers are constructed. The first spacer layer has two important functions: it must provide a non-conducting separation between the silver and the mask and, secondly, it planarises the mask's topology to allow unconfounded superlensing results. To deliver this, a layer of PMMA is spun onto the tungsten pattern coverslip approximately 6-8 times thicker than required. This is then reflowed overnight at 185°C before being gradually etched back to the required thickness. This method planarises 30nm steps in the tungsten

mask to less than 5nm, with a surface roughness of less than 1nm root-mean-square (RMS).

Following this, silver and silicon dioxide layers are deposited by thermal evaporation in a single vacuum deposition run, to avoid oxidation or sulphidation of the silver. The silver deposition process has been developed to provide the smoothest layer possible, which is achieved through fast deposition (see table 7). Below a thickness of 35nm it was found that the silver's roughness greatly increased. Typical roughness values for the silver and silicon dioxide layers are approximately 1nm RMS for the single layer and approximately 2nm RMS for the double layers.

The level of planarisation of the final mask is important so that no imaged features can be attributed to the topography of the silver layer. The final planarisation for all masks is less than 5nm for the results shown here and, for gratings below a 250nm period, it is less than 2.5nm peak-to-peak.

Finally, the coverslip is attached to a rigid glass plate, which adapts the mask stack for use with a Karl S*ü*ss MA-6 mask aligner. A 350W Mercury lamp is used with an i-line (365nm) interference filter, which gives a resultant exposure intensity of 2mW/cm^2. The mask is brought into soft vacuum contact with a silicon substrate that is spun coated with Clariant BARLi-II-200 bottom anti-reflection coating (BARC) and 100nm thick Clariant HiR1075 resist (diluted 1:4 with methyl amyl ketone). The silcon substrates are one-inch diameter p-type wafers that are cleaned with acetone, methanol, and IPA. This cleaning process is very important as dust particles regularly render experiments unuseable. Exposure times are long – ranging from 400-900s – due to the intensity reduction through the interference filter and silver layers. Exposed samples are then developed in full strength AZ300-MIF developer (2.18% tetra-methyl ammonium hydroxide) for 3s, and rinsed in deionised water.

For investigating the performance of the system a Digital Instruments DI3100 atomic force microscope (AFM) has been used to scan the exposed samples. At this stage no pattern transfer has been attempted into the silicon, however this has been proven to work well by Alkaisi *et al.*[9] for a related near-field lithography process.

A. Fabrication issues

There are a number of refined process steps required to achieve unambiguous super-resolution using the PLL method. Some of the limiting factors that result from these processes are: resolution restrictions for gratings using the EBL and RIE patterning process, sufficient planarisation of the first spacer layer, exact control of the first spacer layer's thickness, and

roughness of the silver. These four limitations have restricted or limited our experimental testing.

Our tungsten mask patterning process has a resolution limit of between 100-120nm. This is close to the current limit of the experiments, thus the absolute resolution limit may not have been reached. The limit is mainly due to proximity effects during the EBL patterning of the PMMA, and we are currently investigating ways to overcome this.

When the first spacer layer is planarised, control over the final thickness is difficult. The oxygen RIE process used to etch back the PMMA layer is controllable to ± 3nm, which then puts limits on the stack's following layers, as the ratio of spacer to silver lens is predetermined[3]. This has meant that performing comparisons between single- and double-layered masks with exactly the same total thickness of silver has been difficult.

The silver evaporation process has been tuned to produce the smoothest layers possible, which is achieved through increased deposition rate. This works for film thicknesses greater than 35nm with great success, but below this the roughness of the silver increases. This roughness increase can be attributed to a lack of surface 'wetting', which results in beading due to surface tension. These effects are overcome for thicknesses above 35nm. Thinner layers of the SiO_2 spacer also suffer from pin-holes, which can cause shorts between conducting layers. This has limited us to the study of single- and double-layer lenses, whereas improved performance for larger numbers of layers has been proposed[8]. To allow faster deposition of silver to minimise these problems, a more robust planarisation layer may be required.

3. Experimental Results

Single and double-layered PLL experiments have been carried out and their performance analysed. Initial super-resolution results were produced through a 25/50/10 - PMMA/Ag/SiO_2 lens stack[5] using broadband illumination. These results have been improved on by filtering the broadband light to give an i-line (365nm) narrowband exposure. Figure 2 shows a range of mask periods that have been imaged, with gratings clearly resolved down to a 170nm period. For our experimental setup the diffraction-limit is set at 243nm[11], thus these images demonstrate silver's ability to project a sub-diffraction-limited image in the near field. All features are imaged from a sample that was exposed for 720s, which is six-times the exposure time required for the broadband exposure. Fully developed features in the 100nm resist are found at periods of 700nm and above, but this reduces to a 5nm

exposed depth for sub-diffraction-limited features.

The best resolution to date is for 145nm period gratings, imaged with the 25/50/10 stack in a 720s exposure. Figure 3 shows an AFM scan of the 145nm period features as well as a Fourier transform of an averaged line scan perpendicular to the grating to show the spectral components in the image. This is a large step forward in image fidelity when compared with the previous broadband results[5]. The increase in image fidelity is attributed to the removal of exposing wavelengths (through filtering) that are causing background exposure and low spatial frequency distortion in the patterns. This evident when the spatial spectrum of the narrowband result here (Fig. 3(b)), and the broadband result in Ref[5] are compared. The 145nm period peak in the broadband result is of similar intensity to the low frequency energy, whereas in the narrowband result the 145nm peak's intensity is higher than all other spectral components, leading to a better image.

A double layer mask was constructed to test the hypothesis that a multi-layered stack would improve the resolution and overcome limitations due to imperfections in the stack's layers[8]. The first double layered mask constructed used a 15/30/30/30/10 - PMMA/Ag/SiO_2/Ag/SiO_2 stack. The performance of this mask is compared to the 25/50/10 stack in Fig. 4. The exposure time for the double-layer sample is 420s, which is almost half the length of time required for the exposures through the single 50nm silver layer. This indicates an increase in transmission through the double layer stack despite the increase in total silver thickness. Features above the diffraction limit are imaged with good clarity as seen by the 290nm grating period image in Fig. 4. Sub-diffraction-limited resolution is also found, however image fidelity for the double layer is reduced considerably. This is clearly depicted by the increased granularity in the 200nm and 170nm grating period images compared with their counterparts imaged through the 25/50/10 stack. The reduction in fidelity is the result of increased surface roughness for the double layer stack, so this is a key parameter that must be improved if the use of multi-layer silver lenses is to be explored further. Nonetheless, these results show that a double-layer stack can achieve similar resolution to a thinner single-layer stack, with higher light transmission.

Figure 5 shows the performance of a 30/60/30 - PMMA/Ag/SiO_2 stack that did not produce any sub-diffraction-limited results, but has the same total thickness of silver as the 15/30/30/30/10 stack. This suggests that experimentally a multi-layered mask can achieve better resolution for the same silver thickness. However, the final spacing of 30nm compared

to 10nm confounds these results somewhat; it is generally the case that a thinner final spacer is required in order to project the final image a short distance into the imaging resist layer[5,6]

The increase in the resolution and transmission for the double layer can be attributed to an increase in coupling between the layers. For near-field amplification, the fields in a thicker silver layer require larger amplitudes. Since silver is a lossy medium these larger amplitudes are dissipated, reducing the system's ability to transfer the spatial information. The higher spatial frequencies decay faster as function of distance from the silver surface thus they require more amplification to 're-focus' in the same plane, this leads to the higher spatial frequencies being more highly dissipated. The reduction in amplitude in the thinner silver layers will therefore allow higher spatial frequencies to be transmitted and provide better resolution.

~~In the double layer stack images there is a noticeable reduction in the image fidelity (most noticibly for the 170nm period grattings in Fig 4). This is caused by an increased surface roughness attributed to three effects: Firstly, in the 15/30/30/30/10 stack case roughness is caused by the reduction in the thickness of the silver layers (deposition of silver to a thickness less than 35nm results in rougher films as the granularity due to surface tension and cluster size has not yet been overcome by heating and bombardment); secondly, the two additional interfaces in the double layered stack tend to amplify any defects in the lower layers, compounding the roughness from layer to layer; finally, for the thinner layers there is a greater the likelihood of pin-hole shorts between conducting layers — these shorts dampen the plasmonic effects that the technique relies on.~~

A double layered 25/50/50/50/10 - PMMA/Ag/SiO_2/Ag/SiO_2 PLL stack has also been investigated to compare with our previous experiments of imaging through much thicker silver layers[4,12]. A range of images for a 900s exposure are shown in Fig. 6. No sub-diffraction-limited resolution features were produced from this mask, however, sub-wavelength features were produced that had higher resolution and image fidelity than previous results through 120 and 85nm single silver layers[4,12]. Figure 6 shows images of gratings with sub-wavelength features, but the image fidelity has again been lost due to the increase roughness from the double layers. Although high-spatial frequency features have not been resolved, the mask's performance above 250nm half-pitch sized features is still good; there is low edge line roughness and the pattern is fully developed into the 100nm thick resist layer.

4. Simulation Results

Finite-difference time domain (FDTD) electromagnetic simulations have been used to support the experimental results, to explore the nature of the process, and to predict performance. The details of the simulation techniques that we have employed have been described previously[12]; these simulations showed similar sub-diffraction-limited resolution cutoffs to those experimentally observed for proximity (no lens) and single-layer lens imaging.

Here we present two-dimensional electric intensity simulations for no-lens, single-layer lens, and double-layer lens systems under a 170nm period grating. Figure 7 shows a comparison between a 85nm PMMA proximity spacer, a 25/50/10nm - PMMA/Ag/SiO_2 single-layer lens stack and a 15/30/30/30/10nm - PMMA/Ag/SiO_2/Ag/SiO_2 double-layer lens stack. For the no-lens case (Fig. 7(a)) the limitations of proximity exposure for sub-diffraction-limited features is evident in the lack of contrast in the resist. The ability of single- and double-layer the silver superlenses to project the sub-diffraction-limited source features to an image plane is shown by Figures 7(b) and (c). Traces through these simulations at a depth of 30nm into the resist (as indicated by the dashed line through the images in Fig. 7) are shown in Fig. 8. Here we can see that the proximity case has not managed to transfer the features into the resist, but the superlenses are able to produce clear features. The traces for the double- and single-layer lens also show that we expect higher transmission (about two-times) and better contrast for the double-layer lens, which is what is seen experimentally. At this stage the effect of surface roughness has not been investigated through simulation.

5. Conclusion

This work has demonstrated that super-resolution can be achieved through single- and double-layer of silver imaging stacks in an optical lithography regime. Gratings have been resolved down to a 145nm period for a single layer and to 170nm for a double layer. The resolution limit for a double layer is as good or better than a single layer with the same total silver thickness, however a true limitation on the pattern fidelity has been found due to the increase in surface roughness that is symptomatic of multiple layers. For multiple-layer PLL to achieve commercial quality sub-100nm dense features, work must be carried out to improve the quality of silver films thinner than 30nm. If this is completed, PLL could be a low-cost technique for sub-100nm optical lithography.

6. Acknowledgements

The authors wish to thank Conrad Wolf, Alan Wright, and Andrew Thomson for collaboration and laboratory assistance, Helen Devereux and Gary Turner for technical support, and Dr. Maan Alkaisi for co-supervision. Useful discussions with Hank Smith and James Goodberlet (MIT) are also acknowledged. This research was supported by the Marsden Fund of the Royal Society of New Zealand (contract UOC-312). David also acknowledges the financial support of the University of Canterbury Brownlie Scholarship.

7. Author Contact Information

Please address correspondence to the email address r.blaikie@elec.canterbury.ac.nz.

References

1. J. B. Pendry, "Negative refraction makes a perfect lens," Phys. Rev. Lett. **85**(18), 3966–3969 (2000).
2. S. A. Ramakrishna, "Physics of negative refractive index materials," Rep. Prog. Phys. **68**(2), 449–521 (2005).
3. V. G. Veselago, "The Electrodynamics of Substances with Simultaneously Negative Values of ϵ and μ," Sov. Phys. Usp. **10**(4), 509–514 (1968).
4. D. O. S. Melville, R. J. Blaikie, and C. R. Wolf, "Submicron Imaging With a Planar Silver Lens," Appl. Phys. Lett. **84**(22), 4403–4405 (2004).
5. D. O. S. Melville and R. J. Blaikie, "Super-resolution imaging through a planar silver layer," Opt. Express **13**(6), 2127–2134 (2005).
6. N. Fang, H. Lee, C. Sun, and X. Zhang, "Sub-diffraction-limited optical imaging with a silver superlens," Science **308**(5721), 534–537 (2005).
7. R. J. Blaikie and S. J. McNab, "Simulation study of 'perfect lenses' for near-field optical nanolithography," Microelectron. Eng. **61-62**, 97–103 (2002).
8. S. A. Ramakrishna, J. B. Pendry, M. C. K. Wiltshire, and W. J. Stewart, "Imaging the near field," J. Mod. Opt. **50**(9), 1419–1430 (2003).
9. M. M. Alkaisi, R. J. Blaikie, S. J. McNab, R. Cheung, and D. R. S. Cumming, "Sub-diffraction-limited patterning using evanescent near-field optical lithography," Appl. Phys. Lett. **75**(22), 3560–3562 (1999).
10. J. G. Goodberlet and H. Kavak, "Patterning Sub-50 nm features with near-field embedded-amplitude masks," Appl. Phys. Lett. **81**(7), 1315–1317 (2002).
11. G. O. Reynolds, G. B. Parrent, J. B. DeVelis, and B. J. Thompson, "Resolution in Terms of the Impulse Response," in The New physical optics notebook : tutorials in Fourier optics, p. 38 (Spie Optical Engineering Press ; American Institute of Physics, Bellingham, Wash. New York, N.Y., 1989).
12. R. J. Blaikie and D. O. S. Melville, "Imaging through planar silver lenses in the optical near field," J. Opt. A: Pure Appl. Opt. **7**, S176–S183 (2005).

Table 1. The sputtering conditions used for tungsten deposition.

Target	Power	Rate	Temp.	Process Pressure
W (99.99%)	300W DC	0.24 nm/s	25°C < T < 40°C	8.5e-3 mBar

Table 2. Process parameter table for reactive ion etching of Tungsten and PMMA.

Material	Etch Mask	Etch Rate	Gases	Flow Rate	RF Power	Temp.	Process Pressure
W	PMMA	3.8 nm/s	SF_6	80 sccm	200W	313°K	150 mTorr
PMMA	-	3 nm/s	O_2	40 sccm	100W	295°K	100 mTorr

Table 3. Process parameter table for thermal evapouration of silver and silicon dioxide.

Target	Rate	Process Pressure
Ag (Ag pelets)	2 nm/s	4e-6 Bar
SiO_2 (SiO powder)	0.5 nm/s	4e-6 Bar

Figure Captions

Fig. 1: (Color online) Experimental setup of single- and double-layer planar lens lithography

Fig. 2: (Color online) Atomic force microscope scans of features imaged through a 25/50/10 - PMMA/Ag/SiO_2 stack. Gratings with periods of 500nm through to 170nm are shown, with the 200 and 170nm features achieving sub-diffraction-limited resolution. All height scales are 50nm.

Fig. 3: (Color online) (a) Atomic force microscope scan and (b) associated Fourier transform of an averaged line scan for 145nm period features imaged through a 25/50/10 - PMMA/Ag/SiO_2 stack. The height scale is 50nm.

Fig. 4: (Color online) A comparison of atomic force microscope scans for features imaged below a single-layer 25/50/10 - PMMA/Ag/SiO_2 stack and a double-layer 15/30/30/30/10 - PMMA/Ag/SiO_2/Ag/SiO_2 stack. All height scales are 50nm.

Fig. 5: (Color online) Atomic force microscope scans of features imaged through a 30/60/30 - PMMA/Ag/SiO_2 stack. Periods from 1μm to 350nm are shown. No dense grating features with periods below 350nm were found. All height scales are 50nm.

Fig. 6: (Color online) Atomic force microscope scans of features imaged through a double-layer 25/50/50/50/10 - PMMA/Ag/SiO_2/Ag/SiO_2 stack. Periods from 1μm down to 350nm are shown. No dense grating features with periods below 350nm were found. All height scales are 50nm.

Fig. 7: (Color online) Two-dimensional finite-difference time-domain simulations of (a) a proximity exposure, (b) a single-layer 25/50/10 - PMMA/Ag/SiO_2 stack, and (c) a double-layer 15/30/30/30/10 - PMMA/Ag/SiO_2/Ag/SiO_2 stack.

Fig. 8: (Color online) One-dimensional traces extracted from two-dimensional finite-difference time-domain simulations of double- (15/30/30/30/10 - PMMA/Ag/SiO_2/Ag/SiO_2) and single-layer (25/50/10 - PMMA/Ag/SiO_2) lens stacks. A trace for a 85nm proximity simulation is also provided for comparison. Traces are taken at a depth of 30nm into the resist. The location of the trace is indicated in by the dashed line in Fig. 7.

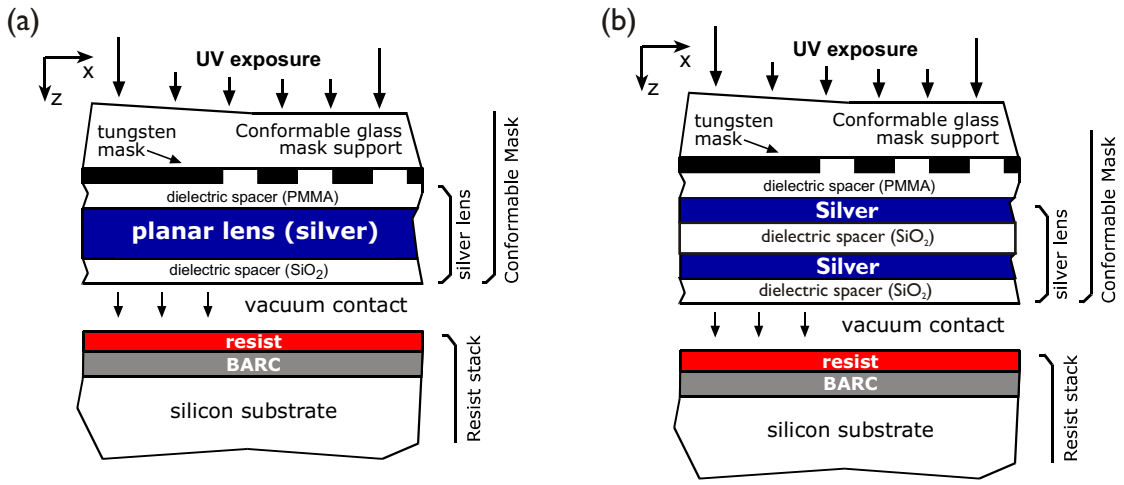

Fig. 1.

Fig. 1 - David O. S. Melville and Richard J. Blaikie. ***Experimental comparison of resolution & pattern fidelity in single- and double-layer planar lens lithography***

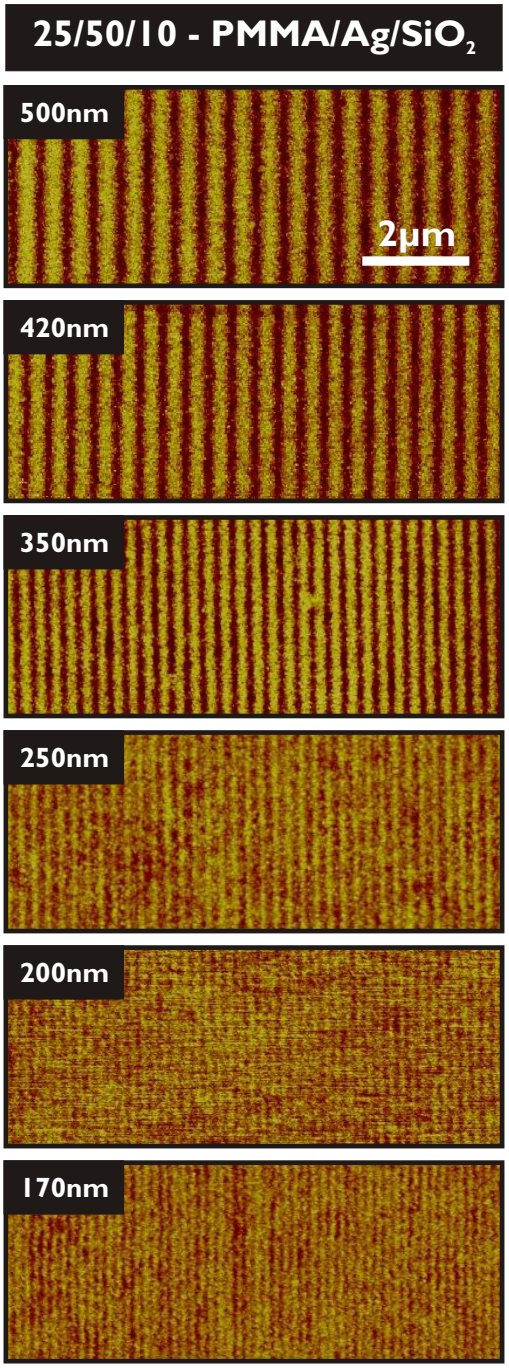

Fig. 2.

Fig. 2 - David O. S. Melville and Richard J. Blaikie. ***Experimental comparison of resolution & pattern fidelity in single- and double-layer planar lens lithography***

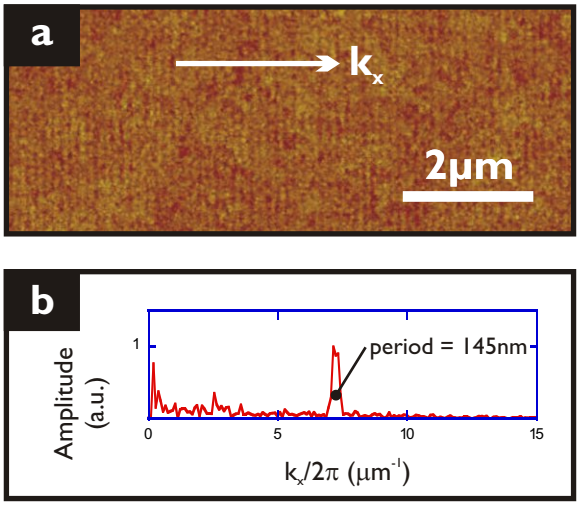

Fig. 3.

Fig. 3 - David O. S. Melville and Richard J. Blaikie. ***Experimental comparison of resolution & pattern fidelity in single- and double-layer planar lens lithography***

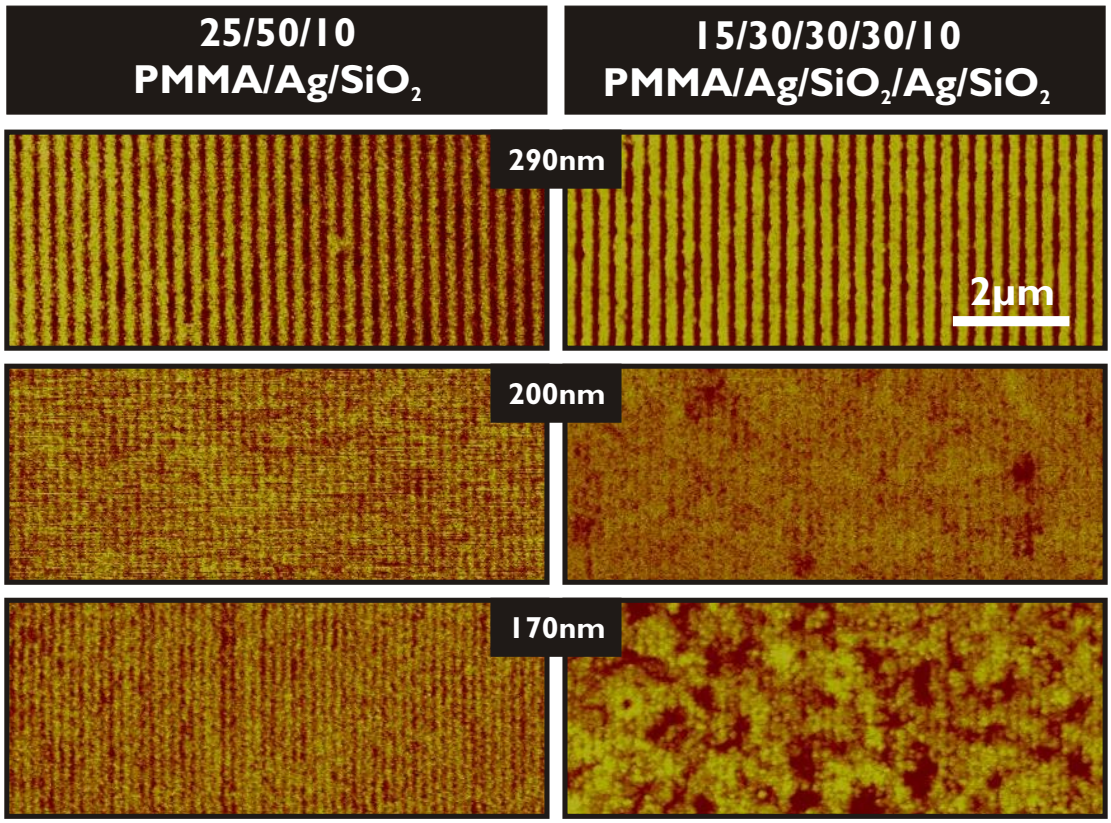

Fig. 4.

Fig. 4 - David O. S. Melville and Richard J. Blaikie. ***Experimental comparison of resolution & pattern fidelity in single- and double-layer planar lens lithography***

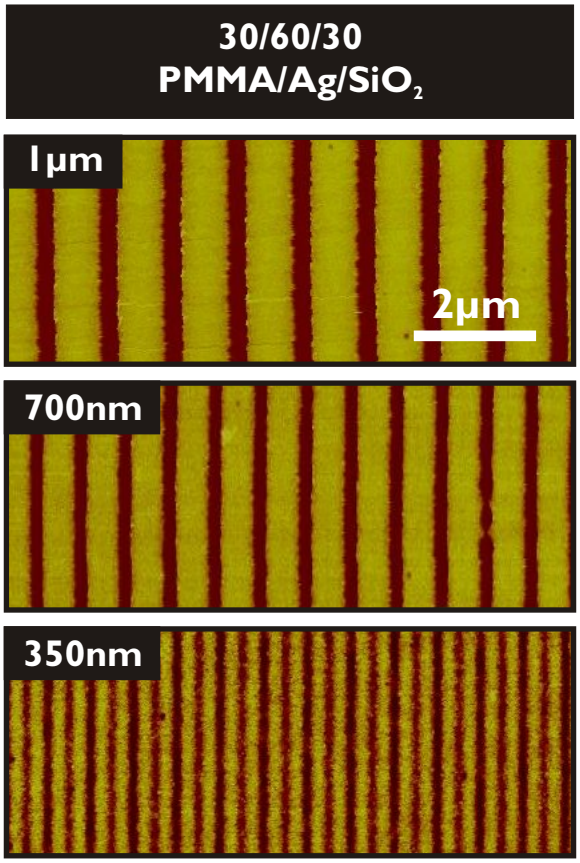

Fig. 5.

Fig. 5 - David O. S. Melville and Richard J. Blaikie. ***Experimental comparison of resolution & pattern fidelity in single- and double-layer planar lens lithography***

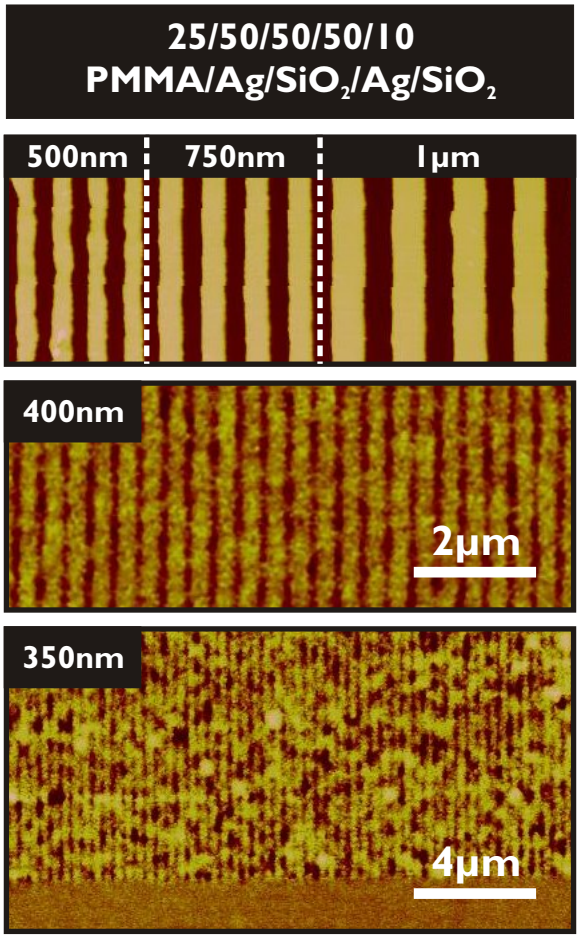

Fig. 6.

Fig. 6 - David O. S. Melville and Richard J. Blaikie. ***Experimental comparison of resolution & pattern fidelity in single- and double-layer planar lens lithography***

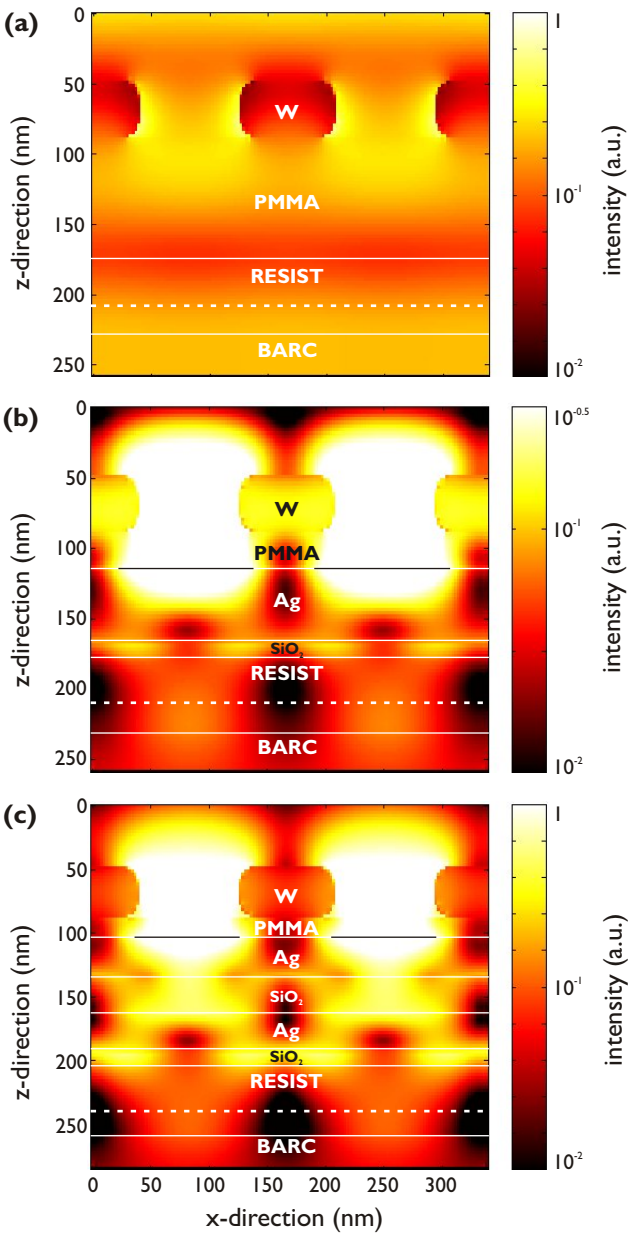

Fig. 7.

Fig. 7 - David O. S. Melville and Richard J. Blaikie. ***Experimental comparison of resolution & pattern fidelity in single- and double-layer planar lens lithography***

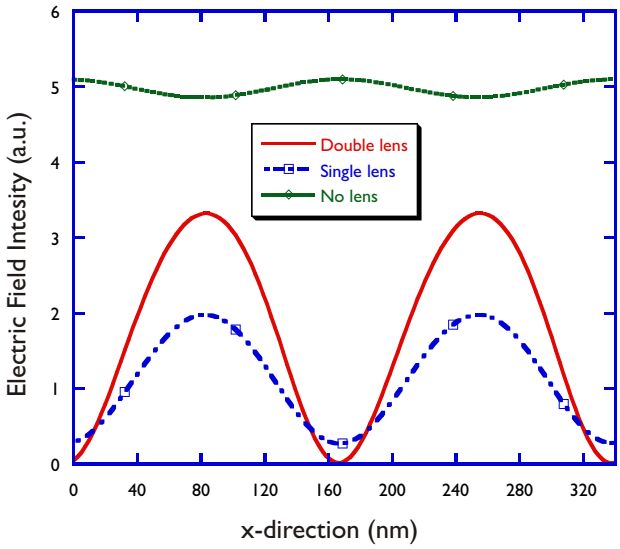

Fig. 8.

Fig. 8 - David O. S. Melville and Richard J. Blaikie. ***Experimental comparison of resolution & pattern fidelity in single- and double-layer planar lens lithography***